Available online at www.sciencedirect.com
SCIENCE DIRECT®
Bioorganic & Medicinal Chemistry Letters 15 (2005) 5274–5279
Bioorganic & Medicinal Chemistry Letters

Two classes of p38α MAP kinase inhibitors having a common diphenylether core but exhibiting divergent binding modes

Enrique L. Michelotti,[a] Kristofer K. Moffett,[a] Duyan Nguyen,[a] Martha J. Kelly,[a] Rupa Shetty,[a] Xiaomei Chai,[b] Katrina Northrop,[b] Variketta Namboodiri,[b] Brandon Campbell,[a] Gary A. Flynn,[a] Ted Fujimoto,[c] Frank P. Hollinger,[c] Marina Bukhtiyarova,[b] Eric B. Springman[b] and Michael Karpusas[b,*]

[a]*Department of Chemistry, Locus Pharmaceuticals, Inc., Four Valley Square, 512 Township Line Rd, Blue Bell, PA 19422, USA*
[b]*Department of Biology, Locus Pharmaceuticals, Inc., Four Valley Square, 512 Township Line Rd, Blue Bell, PA 19422, USA*
[c]*Department of Technology and Informatics, Locus Pharmaceuticals, Inc., Four Valley Square, 512 Township Line Rd,Blue Bell, PA 19422, USA*

Received 24 June 2005; revised 12 August 2005; accepted 15 August 2005
Available online 19 September 2005

Abstract—Two new classes of diphenylether inhibitors of p38α MAP kinase are described. Both chemical classes are based on a common diphenylether core that is identified by simulated fragment annealing as one of the most favored chemotypes within a prominent hydrophobic pocket of the p38α ATP-binding site. In the fully elaborated molecules, the diphenylether moiety acts as an anchor occupying the deep pocket, while polar extensions make specific interactions with either the adenine binding site or the phosphate binding site of ATP. The synthesis, crystallographic analysis, and biological activity of these p38α inhibitors are discussed.

p38α Mitogen-activated protein (MAP) kinase is an intracellular serine-threonine kinase that plays a critical role in the regulation of pro-inflammatory cytokine pathways. Once activated by phosphorylation, p38α sequentially phosphorylates and activates a wide variety of downstream substrates including other protein kinases and transcriptional factors. This ultimately results in significant transcriptional up-regulation of the pro-inflammatory cytokines such as tumor necrosis factor α (TNFα).[1,2] Consequently, the p38α protein kinase has been implicated as a major regulator of inflammatory responses and has therefore been a target of extensive research efforts focusing on development of small molecule inhibitors for the treatment of inflammatory and autoimmune diseases, including rheumatoid arthritis, inflammatory bowel disease, and osteoporosis.

There have been a large number of reports for different classes of p38 inhibitors that are active in vitro and in vivo assays (reviewed in Refs. 2–5). Several inhibitors have progressed into development and clinical trials due to their potential as anti-inflammatory therapeutics.[6] Extensive crystallographic and biochemical studies have provided considerable understanding of the details of binding of several classes of small molecule inhibitors to the p38 ATP-binding site. In one of the first such studies, structures of a series of selective p38 inhibitors based on pyridinylimidazole and pyrimidinylimidazole moieties that were soaked into p38 crystals were described.[7] Of these, inhibitor SB-203580 serves as the prototype for comparing different inhibitor subclasses. A common characteristic of all these inhibitors is that they contain a planar ring system that occupies a position similar to that of the adenine ring of ATP and recapitulates several H-bonds of the adenine ring with the protein. The inhibitors also contain additional groups, interacting with nearby protein regions that have been incorporated in order to improve potency, selectivity, and pharmacokinetics.

Here, we report two new classes of p38α inhibitors based on a key diphenylether moiety and describe their chemical synthesis and biological activity.[8,9] Series 1 is composed of the diphenylether moiety at one end of the molecule attached to an aryl substituent at the opposite

Keywords: p38α kinase; MAP kinase; ATP site; X-ray; Crystal.
* Corresponding author. Tel.: +1 215 358 2074; fax: +1 215 358 2030; e-mail: mkarpusas@locuspharma.com

0960-894X/$ - see front matter © 2005 Elsevier Ltd. All rights reserved.
doi:10.1016/j.bmcl.2005.08.038

end of the molecule via an amide linker (Fig. 1). Series 2 is composed of a diphenylether moiety at one end of the molecule but is attached via a sulfamide substructure to a 4-amino-piperidine (Fig. 2). Series 2 is further extended to include an aryl substituent attached to the 4-amino group of the piperidine. The diphenylether scaffold was identified by a fragment-based computational methodology and incorporated into a chemical strategy focused on the discovery of new chemical classes of inhibitors.[10–12]

Compounds **1a**–**1h** (Fig. 1) were prepared from commercially available amines and substituted 4-phenoxybenzoic acids by standard coupling chemistry using EDCI and HOBt in CH_2Cl_2. The amine portion of compounds **1b** and **1h** was prepared from 3-hydroxyphenylacetic acid using the Claisen rearrangement as the key step to introduce the quaternary center. The amine functionality was achieved using a Curtius-type rearrangement using diphenylphosphoryl azide. TIPS and Boc removal was followed by standard amide coupling conditions and subsequent exposure to $BF_3{\cdot}Et_2O$ to give the desired product (see Supporting information).

Compounds **2a**–**2h** (Fig. 2) were prepared from 4-aminopiperidine employing *N*,*N*′-sulfuryldiimidazoles as key intermediates (Scheme 1).[15] Treatment of 4-*N*-Boc-aminopiperidine with triflate **3** provided Boc-protected imidazo piperidine **4** which after treatment with methyl trifluorosulfonate followed by the corresponding phenoxyaniline and Boc removal afforded sulfamide **6** with moderate yields. Targeted compounds **2** were easily prepared by reductive amination of **6** and the corresponding benzaldehyde (Scheme 1 and Supporting information).

Both chemical classes inhibit the measured enzymatic activity of p38α.[9] A limited structure–activity profile was generated for each of the two diphenylether-based inhibitor classes. In compounds of Series 1, modification of the diphenylether group of compound **1b** to include a

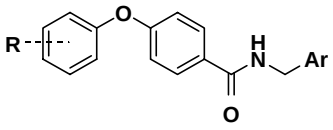

Compound	R	Ar	IC_{50} (μM)
SB-203580	-	-	0.29
1a	H	2-pyridyl	1.5
1b	H	3-hydroxy-4-(1-hydroxy-2-methylpropan-2-yl)phenyl	1.6
1c	H	p-tolyl	1.6
1d	H	4-trifluoromethylphenyl	1.4
1e	H	5-indanyl	1.2
1f	H	3-trifluoromethoxyphenyl	0.6
1g	H	3-trifluoromethylphenyl	0.45
1h	4-Cl	3-hydroxy-4-(1-hydroxy-2-methylpropan-2-yl)phenyl	0.4

Figure 1. Structure–activity relationship of diphenylether Series 1 inhibitors.

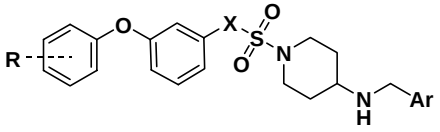

Compound	R	X	Ar	IC_{50} (μM)	% inhibition
SB-203580	-	-	-	0.29	-
2a	4-F	N	2-Phenol	6.0	-
2b	2,4-diF	N	2-Phenol	10.0	-
2c	H	N	2-Phenol	16.0	-
2d	2-Cl	N	2-Phenol	>20.0	37
2e	3-CF_3	N	2-Phenol	>20.0	27
2f	H	N	Phenyl	>20.0	21
2g	H	N	1-Napthyl	>20.0	24
2h	H	C	2-Phenol	>20.0	0

Figure 2. Structure–activity relationship of diphenylether Series 2 inhibitors. The numbers of the last column on the right indicate percent inhibition at a concentration of 10 μM.

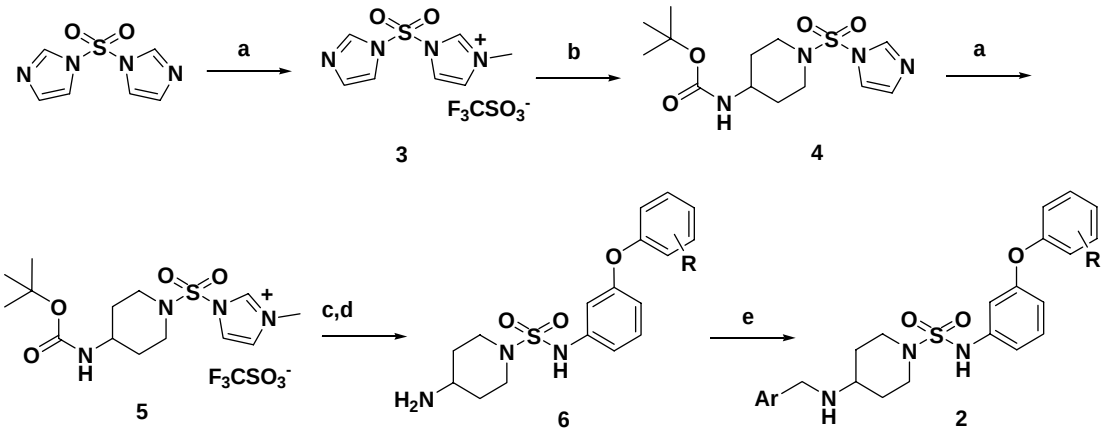

Scheme 1. Preparation of compounds of series **2**.

4-chloro substituent, compound **1h**, increases potency by 3- to 4-fold. Modification of the aryl group opposite the diphenylether of compounds, such as **1a** or **1b**, to a more hydrophobic moiety, particularly a 3-substituent group such as in **1f** and **1g**, increases potency 2- to 3-fold.

In compounds of Series 2, addition of a 4-fluoro group (compound **2a**) (Fig. 2) to the diphenylether results in a 2- to 3-fold increase in potency, while substituents in the 2 and 3 positions appear to be unfavorable. Removal of the phenol hydroxyl of compound **2c** results in a significant loss in activity (compound **2f**), suggesting that this substituent plays an important role in binding. Modification of the sulfamide linker of compound **2c** to a sulfonamide linker (compound **2h**) results in a complete loss of measurable activity.

In order to facilitate an understanding of these structure–activity relationships, four p38α inhibitor complexes (with representative compounds **1a**, **1h**, **2a**, and **2c**, respectively) were crystallized and the X-ray crystal structures were determined to 2.0–2.5 Å resolution (see Supporting information, Table 1).[13] Inhibitors from both Series 1 and Series 2 are observed to bind in the general vicinity of the ATP-binding site of the kinase molecule, which is consistent with the observation that both series of inhibitors are ATP-competitive (Figs. 3 and 4). The diphenylether moiety of both series is observed to adopt a common binding mode. It is buried in a predominantly hydrophobic pocket (referred to as pocket I) formed by residues Ala51, Lys53, Leu75, Ile84, Leu104, Thr106, and Leu167. Extensive van der Waals and hydrophobic contacts characterize the interactions between the inhibitors and the protein residues forming this pocket. The positions of the two aromatic rings that comprise the diphenylether moiety are very similar to those of two aromatic rings of SB-203580 (PDB entry 1A9U).[7] The proximal ring of the diphenylether occupies a position similar to that of the adenine ring of ATP. A C–H···O bond may also be present between this ring of the diphenylether and the main chain carbonyl of His107.[14] The distal ring of the diphenylether, occupying hydrophobic pocket I, is sandwiched between the side-chain atoms of Thr106 and Lys53.

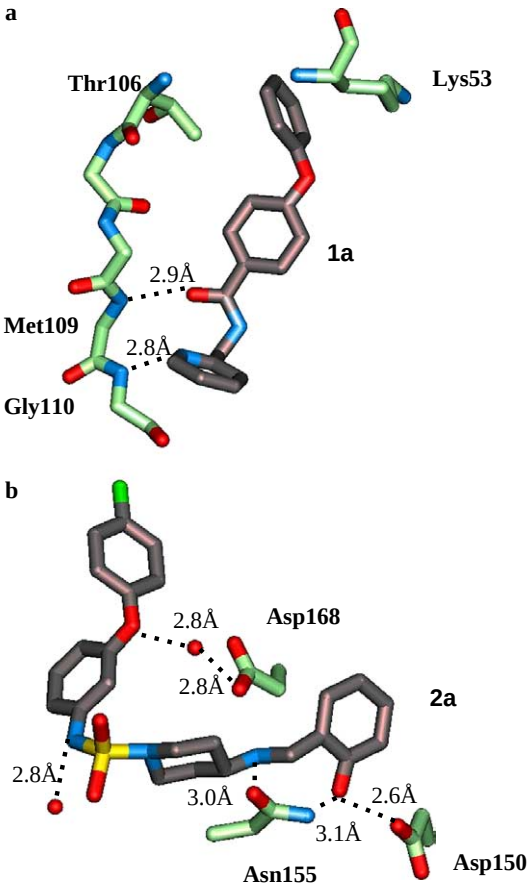

Figure 3. Crystallographically observed binding interactions with p38α for compounds **1a** (a) and **2a** (b). Compound C atoms are colored gray and protein C atoms are colored green. Dotted lines indicate hydrogen bonds and their lengths.

Beyond the diphenylether group, the two series diverge in how they interact with the p38α protein. In Series 1, the amide linker and the distal aryl group (Ar in Fig. 1) of **1a** and **1h** form mainly polar interactions with backbone atoms of the so-called 'hinge' region of p38α (His107-Ala111) similar to those formed by the adenine region of ATP. Specifically the main chain amide NH of

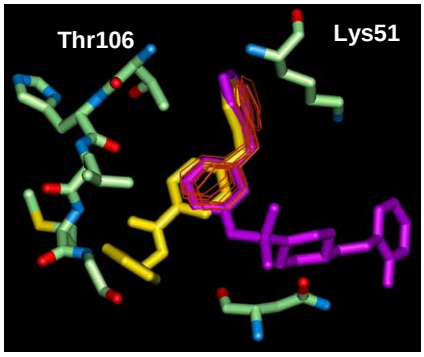

Figure 4. Comparison of compound binding modes after least-squares superimposition of corresponding protein structures. Representative compounds **1a** (yellow) and **2c** (magenta) are compared with each other and with computational predictions for the binding of the diphenylether fragment (thin lines in orange).

Met109 acts as a hydrogen bond donor to the carbonyl oxygen of the inhibitors (Fig. 3). In addition, the amide NH of Gly110 forms a hydrogen bond with the pyridine nitrogen of **1a**.

The portion of the Series 2 compounds distal to the diphenylether forms no interactions with the hinge and occupies a position similar to that occupied by the ribose group and triphosphate chain of ATP (Figs. 3 and 4). The phenol hydroxyl group forms hydrogen bonds with the side chains of Asn158 and Asp168 of the DFG motif as well as hydrophobic contacts with the N-terminal end of the activation loop (Fig. 3). In addition, a hydrogen bond between the Oδ1 of Asn155 and an amine group of the inhibitor is evident. Several water molecules also participate in the formation of a network of hydrogen bonds.

The structure–activity relationships described above are consistent with the interactions observed in the crystal structures of the complexes. Significant variations in the aryl group of Series 1 appear to have a limited effect on enzymatic activity, apparently due to extensive exposure of the group to the solvent and the lack of productive interactions. In contrast, small variations of the diphenylether group appear to have considerable effects. As seen in the crystal structure of **1h**, the Cl atom of the distal diphenylether ring optimizes the van der waals contacts in hydrophobic pocket I and may therefore be responsible for the 4-fold improvement in affinity (IC_{50} = 0.4 μM) with respect to compound **1b** for which the Cl atom is absent (IC_{50} = 1.6 μM). Similarly, the fluorine atom on the diphenylether of **2a** improves the space filling in hydrophobic pocket I with respect to compound **2c**. Examination of the crystal structure indicates that even larger groups than the Cl can be accommodated in that region of the pocket. Due to the tightness of the pocket, the possibilities for additional enhancement of the van der waals contacts by attaching groups in other than the 4-position of the distal diphenylether ring are limited. Indeed, a limited set of compounds that contain attached hydrophobic groups to the diphenylether (**2b**, **2d**, and **2e**) show little change in inhibitory activity.

The observed binding mode of the diphenylether moiety is consistent with the most favored diphenylether fragment distribution identified by analysis of the grand canonical simulated annealing simulation (Fig. 4a).[10,11] The simulation predicts a promiscuity of the pocket for aromatic groups, with the observed diphenylether binding mode being prominent among the predictions. In addition, the computational prediction does not seem to be affected by small conformational differences in the pocket due to the use of the p38 structure coordinates from a different crystal form (PDB entry 1p38). This analysis, together with the observation of the significant effect of small variations to the diphenylether of Series 2 in inhibitory activity, suggests that the diphenylether is an important contributor to inhibitor binding. The extent of hydrophobic contacts between the diphenylether and the surrounding residues of hydrophobic pocket I, allows this moiety to serve as an anchor in the pocket. Thus, the diphenylether is a key pharmacophore element for the two inhibitor series reported here.

Series 2 inhibitors adopt a binding mode that resembles the shape of the letter 'L' with an approximate 99° angle between the distal diphenyl ring, the sulfonamide, and the piperidine rings (Figs. 3 and 4). This shape is determined in part by the conformational preference of the aryl-sulfamide substructure. Conformational energy computations for compound **2c** using the Dihedral Driving module in Maestro software (Schrodinger, LLC) indicate that the angles observed for the N–S–N bonds in the crystal structure are close to their torsional minima. This is supported by the observed structure–activity relationship suggesting that changing the aniline nitrogen of the aryl-sulfamide (**2c**) to carbon (**2h**) results in complete loss of measurable activity. The crystal structures of Series 2 compounds indicate that neither the aniline-nitrogen nor the sulfonamide moiety in compounds, such as **2a** is directly interacting with the protein. The importance of the sulfamide moiety to the p38 inhibitory activity of this series is likely due to the favorable conformation it imposes between the diphenylether and the piperidine rings which redirects the remainder of the molecule toward the activation loop. Another contributor to the unusual conformation of Series 2 inhibitors may be polar interactions of the distal phenol group. The observed loss in activity due to removal of the phenol hydroxyl group for compound **2f** (vs. **2c**) can be explained by the apparent loss of the two H-bonds between the OH group with the side chains of Asn158 and Asp168 (Fig. 3).

In the co-crystal structures of both **2a** and **2c**, the glycine-rich loop (residues # 30–37) has well-defined electron density and has been modeled. It is known that this loop acts as a flexible clamp stabilizing the phosphate groups of ATP. Its apparent stabilization in the complexes with Series 2 inhibitors as opposed to Series 1 may be a result of van der Waals and hydrophobic contacts between the inhibitors and residue Tyr35. In series 2, the side chain of Tyr35 lies under the Gly loop and is stacked against the inhibitor. An internal H-bond is observed between the hydroxyl of Tyr35 and the main chain amide of Ser32 which may also contribute to the

stability. It is also possible that the inhibitor reduces the extent of the disorder by blocking a region of the available space into which the loop would have been free to move. In addition, there is an extensive network of hydrogen bonds facilitated by water molecules which could play a role in binding and stabilization of the glycine-rich loop. In particular, a water molecule simultaneously interacts with Lys53, Glu71, and the diphenylether oxygen of the Series 2 inhibitors (Fig. 3).

In conclusion, we have identified two new and distinct classes of p38α inhibitors and characterized their binding mode by using crystallographic, biochemical, and computational analysis. The similarities in the binding modes of these two inhibitor classes, the structure–activity relationships as well as the computational simulations indicate that the diphenylether motif may be an important pharmacophore element within the p38α ATP-binding site. The remaining portions of the two inhibitor classes reported here have mixed character and adopt conformations that are determined by the intramolecular conformational preference as well as intermolecular interactions. Although the two chemical classes presented here share several characteristics with those of previously reported inhibitors, they also provide new scaffolds for development of new p38α inhibitor classes.

Acknowledgments

We thank Randy Abramowitz and XiaoChun Yang of beamline X4A of the National Synchrotron Light Source, Brookhaven National Laboratory, for assistance with X-ray data collection, and Arifa Husain, Judith Lalonde, and Kendal Williams for comments on the manuscript.

Supplementary data

Supplementary data associated with this article can be found in the online version at doi:10.1016/j.bmcl.2005.08.038.

References and notes

1. Herlaar, E.; Brown, Z. *Mol. Med. Today* **1999**, *5*, 439.
2. Lee, J. C.; Kumar, S.; Griswold, D. E.; Underwood, D. C.; Votta, B. J.; Adams, J. L. *Immunopharmacology* **2000**, *47*, 185.
3. Lee, J. C.; Kassis, S.; Kumar, S.; Badger, A.; Adams, J. L. *Pharmacol Ther* **1999**, *82*, 389.
4. Cirillo, P. F.; Pargellis, C.; Regan, J. *Curr. Top. Med. Chem.* **2002**, *2*, 1021.
5. Adcock, I. M.; Caramori, G. *BioDrugs* **2004**, *18*, 167.
6. Han, J.; Lee, J. D.; Bibbs, L.; Ulevitch, R. J. *Science* **1994**, *265*, 808.
7. Wang, Z.; Canagarajah, B. J.; Boehm, J. C.; Kassisa, S.; Cobb, M. H.; Young, P. R.; Abdel-Meguid, S.; Adams, J. L.; Goldsmith, E. J. *Structure* **1998**, *6*, 1117.
8. *Analytical chemistry:* The compounds are more than 95% pure as verified by analytical reverse-phase high-pressure liquid chromatography (HPLC) and supercritical fluid chromatography.
9. *Procedure for enzymatic assay:* The ATPase activity of activated p38α was determined using a EnzCheck phosphate assay kit (Molecular Probe, OR, USA). The reactions were carried out at 30 °C in 0.1 M Hepes buffer, pH 7.6, containing 10 mM $MgCl_2$ and 10% glycerol. Unless otherwise indicated, the phosphorylated p38α concentrations (Upstate, NY, USA) were maintained at 100 nM. Test compounds and controls were dissolved in DMSO and then diluted with reaction buffer such that the final DMSO concentration in enzymatic reaction was 1%. Compounds were preincubated with p38α for 15 min and enzymatic reactions were initiated by the addition of 1 U/mL nucleoside phosphorylase, 200 μM nucleoside substrate (MESG), and 150 μM ATP. The kinetic analyses were conducted in a 96-well plate on a Molecular Devices spectrophotometer (Molecular Devices Corporation, CA, USA). The IC_{50} was defined as the concentration of the test compound that caused a 50% decrease in the maximal inhibition of p38α activity and was calculated using GraphPad Prizm software.
10. Guarnieri, F. U.S. Patent No. 6,735,530 issued May 11, 2004, 2004.
11. Moore, W. R. *Curr. Opin. Drug Discovery Dev.* **2005**, *8*, 1.
12. *Procedure for fragment annealing computational simulations:* Computations for predicting fragment binding modes were carried using a modification of previously reported methods based on simulated annealing of chemical potential as computed using a grand canonical ensemble.[10,11,16,17] Briefly, the coordinates of the published crystal structure of apo-p38 (1P38) were prepared for computations by adding hydrogens and minimizing rotor states. Binding of the diphenylether fragment to the p38 molecular surface was analyzed by computational simulated annealing over the entire surface. The simulation produced an ensemble of equipotent poses (i.e., a fragment distribution) within the hydrophobic pocket of the ATP-binding region along with the energy associated with the fragment distribution.
13. *Procedure for crystallography:* p38α protein expression using *E. coli* Rosetta™ DE3 host strain, purification, and crystallization has been described previously.[18] For the crystallization, protein/inhibitor complex solution was mixed with reservoir solution (10–20% PEG 4000, 0.1 M cacodylic acid, pH 6, and 50 mM *n*-octyl-β-D-glucoside) at a 3:2 protein/solution volume ratio. Hanging or sitting drops of the mixture were placed over the reservoir solution and crystals were grown by vapor diffusion at 20 °C. For cryoprotection, crystals were gradually transferred to a solution of 18% ethylene glycol, 25% PEG 4000, and 0.1 M cacodylic acid, pH 6, and were flash-frozen in liquid nitrogen. X-ray diffraction data were collected at 100 K, at the X4A beamline of the National Synchrotron Light Source (Upton, NY). Analysis of diffraction data using the HKL program package[19] indicated that the crystals are orthorhombic, of space group $P2_12_12_1$ and approximate cell dimensions 67.7, 70.5, and 76.3 Å. The crystal structures of the p38/inhibitor complexes were solved by molecular replacement and difference Fourier map techniques and refined with the CNX program package (Ref. 20 and Accelrys, Inc.) (Table 1, supporting information). Atomic coordinates with ID codes 1ZYJ and 1ZZ2 have been deposited in the RCSB Protein Data Bank.
14. Cherry, M.; Williams, D. H. *Curr. Med. Chem.* **2004**, *11*, 663.
15. Beaudoin, S.; Kinsey, K. E.; Burns, J. F. *J. Org. Chem.* **2003**, *68*, 115.
16. Mezei, M. *Mol. Phys.* **1987**, *61*, 565.
17. Guarnieri, F.; Mezei, M. *J. Am. Chem. Soc.* **1996**, *118*, 8493.

18. Bukhtiyarova, M.; Northrop, K.; Chai, X.; Casper, D.; Karpusas, M.; Springman, E. *Protein Expr. Purif.* **2004**, *37*, 154.
19. Otwinowski, Z.; Sawer, L. In: isaacs, N.; Bailey, S. eds., Daresbury Laboratory, Warrington, U.K., 1993.
20. Brunger, A. T.; Adams, P. D.; Clore, G. M.; DeLano, W. L.; Gros, P.; Grosse-Kunstleve, R. W.; Jiang, J. S.; Kuszewski, J.; Nilges, M.; Pannu, N. S.; Read, R. J.; Rice, L. M.; Simonson, T.; Warren, G. L. *Acta Crystallogr. D Biol. Crystallogr.* **1998**, *54*(Pt. 5), 905.